CHAPTER VI
NON-ISOTHERMAL MELT-CRYSTALLIZATION AND SUBSEQUENT MELTING BEHAVIOR OF PIGMENTED MEDIUM-DENSITY POLYETHYLENE

6.1 Abstract

Non-isothermal melt-crystallization and subsequent melting behavior of neat MDPE and MDPE filled with three types of pigment (i.e. quinacridone, phthalocyanine, and diarylide) in various amounts ranging between 0.1 and 0.4 phr were investigated using differential scanning calorimetry. The cooling rate range investigated was between 5 and 30°C min^{-1}. For each type of sample investigated, the crystallization exotherm became wider and shifted towards a lower temperature range with increasing cooling rate. All of the pigments investigated were able to shift the crystallization exotherm towards a higher temperature range. Among the various pigments, phthalocyanine was the best in shifting the crystallization exotherm towards a higher temperature range, followed by quinacridone and diarylide, respectively. However, diarylide was the only pigment that was effective in accelerating the crystallization processes of the filled polymer.

6.2 Introduction

Crystallization kinetics of semi-crystalline polymers has continuously been the subject of intense research for many decades. It is now general knowledge that primary crystallization of semi-crystalline polymers comprises mainly the primary and the secondary nucleation mechanisms. A simple way for enhancing the overall crystallization rate of semi-crystalline polymers during processing is by the introduction of a heterogeneous substance that could induce the formation of nuclei. Substances that can induce the formation of nuclei very effectively are called clarifying

and nucleating agents. Pigments are used to impart desirable colors to the final plastic products but, in many cases, they could have a large effect on the crystallization behavior of the plastic during processing. Suzuki and Mizuguchi [1] reported that mold shrinkage or product distortion was always found for colored plastics.

Furthermore, for the crystallization of isotactic polypropylene (iPP), which exhibits several crystal modifications, such as the monoclinic α, the hexagonal β, and the triclinic γ forms, the presence of some pigments, e.g. quinacridone, could promote the formation of the thermally less stable β rather than the thermally more stable α form. A number of authors [2–6] have reported the effect of different types of pigments on crystallization behavior and morphology of iPP.

In the present contribution, the effect of three types of pigments, i.e. quinacridone, phthalocyanine, and diarylide, on non-isothermal melt-crystallization behavior of medium-density polyethylene (MDPE) was investigated by thermal analysis. The kinetics of the non-isothermal melt-crystallization process was analyzed based on the well-known Avrami macrokinetic model.

6.3 Theoretical Background

In differential scanning calorimetry (DSC), the energy released during a non-isothermal crystallization process appears to be a function of temperature. As a result, the relative crystallinity as a function of temperature $\theta(T)$ can be formulated as

$$\theta(T) = \frac{\int_{T_0}^{T} (\mathrm{d}H_c/\mathrm{d}T')\mathrm{d}T'}{\Delta H_c}, \tag{6.1}$$

where T_0 and T represent the onset and an arbitrary temperature, respectively, $\mathrm{d}H_c$ is the enthalpy of crystallization released during an infinitesimal temperature range $\mathrm{d}T$, and ΔH_c is the total enthalpy of crystallization for a specific cooling condition.

To use Eq. (6.1) in analyzing non-isothermal crystallization data obtained by DSC, it is assumed that the sample experiences a similar thermal condition as designated by the DSC oven. This can only be realized when the difference between the temperatures of the sample and the oven is minimal. If this condition is valid, the relation between the crystallization time t and the sample temperature T can be written as

$$t = \frac{T_0 - T}{\phi}, \tag{6.2}$$

where T_0 is an arbitrary temperature and ϕ is the cooling rate. According to Eq. (6.2), the horizontal temperature axis observed in a DSC thermogram for the non-isothermal crystallization data can be transformed into the time domain.

The Avrami model [7–9] is the most common approach for describing the overall isothermal crystallization kinetics. In this model, the relative crystallinity as a function of time $\theta(t)$ can be expressed as

$$\theta(t) = 1 - \exp\left[-(K_A t)^{n_A}\right], \tag{6.3}$$

where K_A and n_A are the Avrami rate constant and the Avrami exponent, respectively. Both K_A and n_A are constants specific to a given crystalline morphology and type of nucleation for a particular crystallization condition [10]. It should be noted that the units of K_A are given as the inverse of time. Although the Avrami equation is often used to describe the isothermal crystallization behavior of semicrystalline polymers, it has also been applied to describe the non-isothermal crystallization behavior of semi-crystalline polymers [11–13].

6.4 Experimental

6.4.1 Materials

The medium-density polyethylene (MDPE) resin used in this work had a density of 0.938 g cm^{-3} and a melt flow rate of 4.0 g/10 min. Three types of pigments used were diarylide or 'Pigment Yellow 83' (C.I.21108; hereafter denoted PY), phthalocyanine or 'Pigment Blue 15' (C.I.74160; hereafter denoted PB), and quinacridone or 'Pigment Red 122' (C.I.73915; hereafter denoted PR), respectively. The chemical structures of these pigments are illustrated in Fig. 6.1.

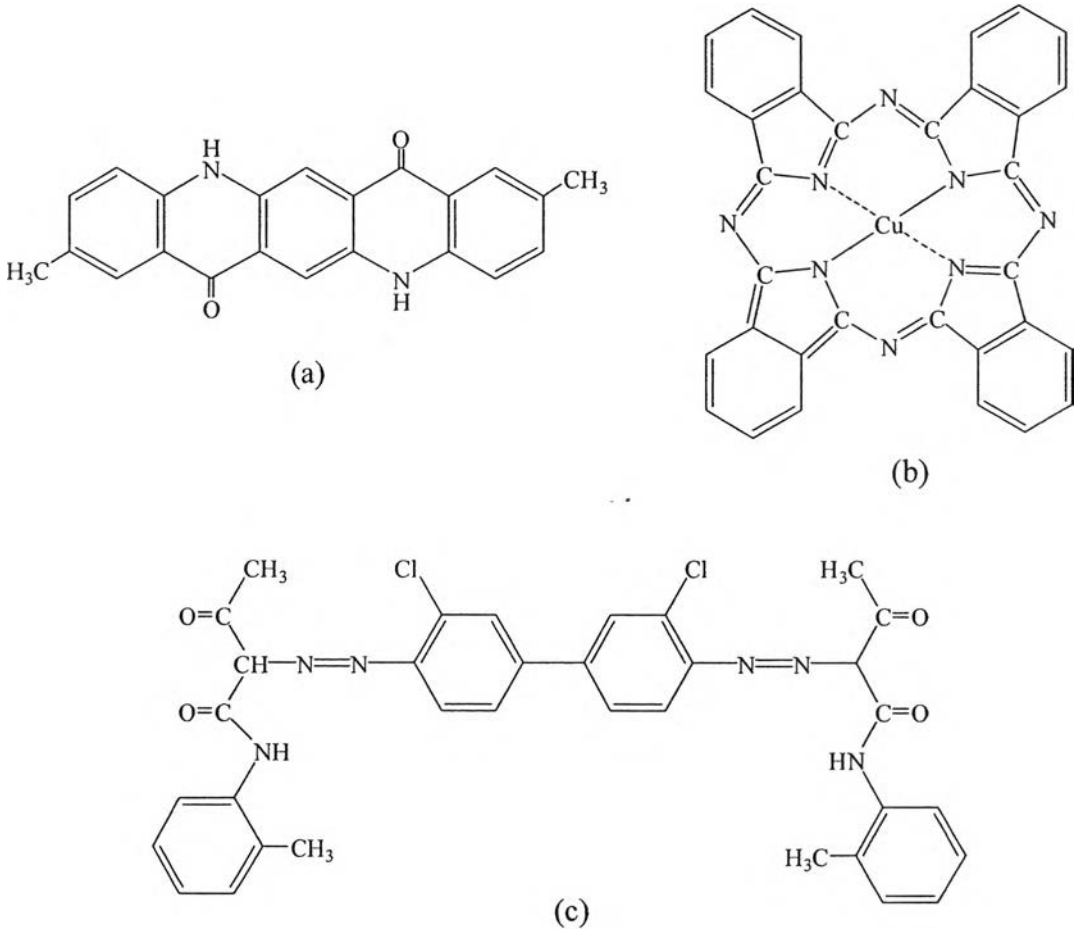

Figure 6.1 Chemical structure of the three pigments investigated: (a) quinacridone or 'Pigment Red 122', (b) phthalocyanine or 'Pigment Blue 25', and (c) diarylide or 'Pigment Yellow 83'.

6.4.2 Sample Preparation

MDPE and each pigment were pre-mixed in a paint mixer. Each pigment was added into MDPE at a content of 0.1, 0.2, 0.3, or 0.4 phr. Both neat MDPE and the pre-mixed formulations were then fed into a Collin ZK25 self-wiping, counter-rotating twin screw extruder, operating at a screw speed of 30 rpm and die temperature of 180°C. All of the samples were then compressed into thin films between a pair of transparency films, which were later sandwiched between a pair of stainless steel platens in a Wabash V50H compression press at 180°C under an applied clamping force of 10 ton-force for 2 min. From this point on, each sample was given an internal code to reflect the type and the content of the pigment incorporated in MDPE: for examples, 'PR01' means MDPE which was added with Pigment Red at a content of 0.1 phr.

6.4.3 Differential Scanning Calorimetry Measurements

A Mettler-Toledo DSC822^e differential scanning calorimeter (DSC) was used to study the non-isothermal melt-crystallization and subsequent melting behavior of neat and pigmented MDPE samples. Calibration for the temperature scale was carried out with a neat indium standard (T_m^0=156.6°C and ΔH_f^0=28.5 J g^{-1}) on every other run to ensure accuracy and reliability of the data. To minimize thermal lag between the polymer sample and the DSC oven each sample holder was loaded with a disc-shaped sample (4.0±0.8 mg) cut from the film samples. Each sample was used only once and all the runs were carried out under nitrogen atmosphere. The measurements started with heating each sample from 25 to 160°C at a heating rate of 80°C min^{-1}. This procedure was to set a similar thermal history for all of the samples investigated. To ensure complete melting, each sample was melt-annealed at 160°C for 5 min, after which time the sample was cooled at a desired cooling rate f, ranging from 5 to 30°C min^{-1}, to 25°C. The subsequent melting behavior was then observed by reheating the sample at a heating rate of 20°C min^{-1} to 160°C. Both non-isothermal melt-crystallization exotherms and subsequent melting endotherms were recorded for further analysis.

6.5 Results and Discussion

6.5.1 Non-Isothermal Melt-Crystallization and Subsequent Melting Behavior

Non-isothermal melt-crystallization exotherms of PB01 at six different cooling rates, ranging from 5 to 30°C min^{-1}, are shown in Fig. 6.2. Clearly, the crystallization exotherm became wider and shifted to a lower temperature with increasing cooling rate, while the melting endotherm was not found to be affected by the cooling rate used. This observation on the crystallization exotherms is attributed to the kinetic effect, which is normally found for crystallization in a nucleation-controlled region. Other samples, including neat MDPE resin, also behaved in a similar way to that observed for PB01. Based on these exotherms, some quantitative data, viz. the temperature at 1% relative crystallinity $T_{0.01}$, the temperature at the maximum crystallization rate or the crystallization peak temperature T_p, and the temperature at 99% relative crystallinity $T_{0.99}$, can be obtained and the results are summarized in Table 6.1. Obviously, these values shifted towards a lower temperature value with increasing cooling rate. It should be noted that $T_{0.01}$ and $T_{0.99}$ represents the onset and the ending points of the non-isothermal melt-crystallization process in the temperature domain.

According to the data shown in Table 6.1, all of the $T_{0.01}$, T_p and $T_{0.99}$ values were found to slightly shift to a higher temperature upon the addition and with increasing content of the different pigments. Among the various pigments investigated, phthalocyanine (PB) was the best in shifting the characteristic values for non-isothermal crystallization, followed by quinacridone (PR) and diarylide (PY), respectively. Fig. 6.3 shows both nonisothermal melt-crystallization exotherms for a fixed cooling rate of 10°C min^{-1} and corresponding subsequent melting endotherms, which were recorded at a fixed heating rate of 20°C min^{-1}, of neat and pigmented MDPE samples. Obviously, all of the pigmented MDPE samples crystallized at a higher temperature region than neat MDPE, suggesting that these pigments acted as nucleating agents for MDPE.

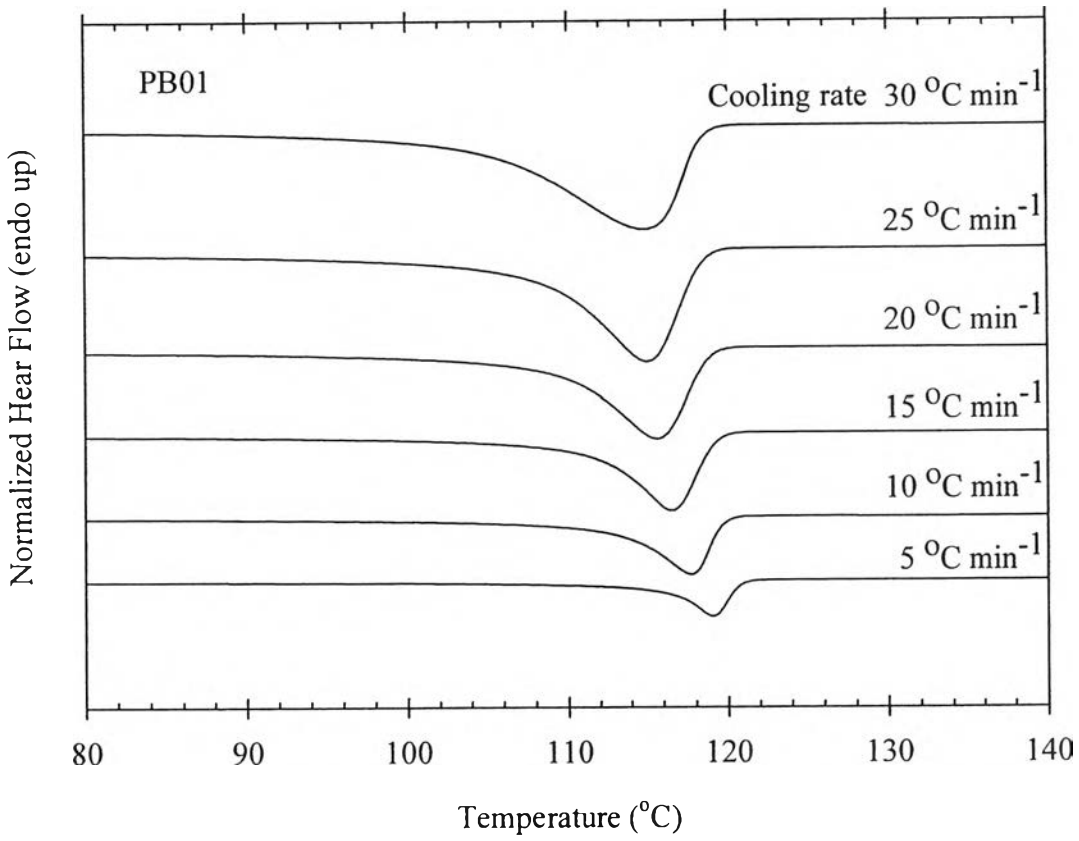

Figure 6.2(a) Non-isothermal melt-crystallization exotherm of MDPE filled with 0.1 phr of phthalocyanine (PB01) at six different cooling rates ranging from 5 to 30°C min^{-1}

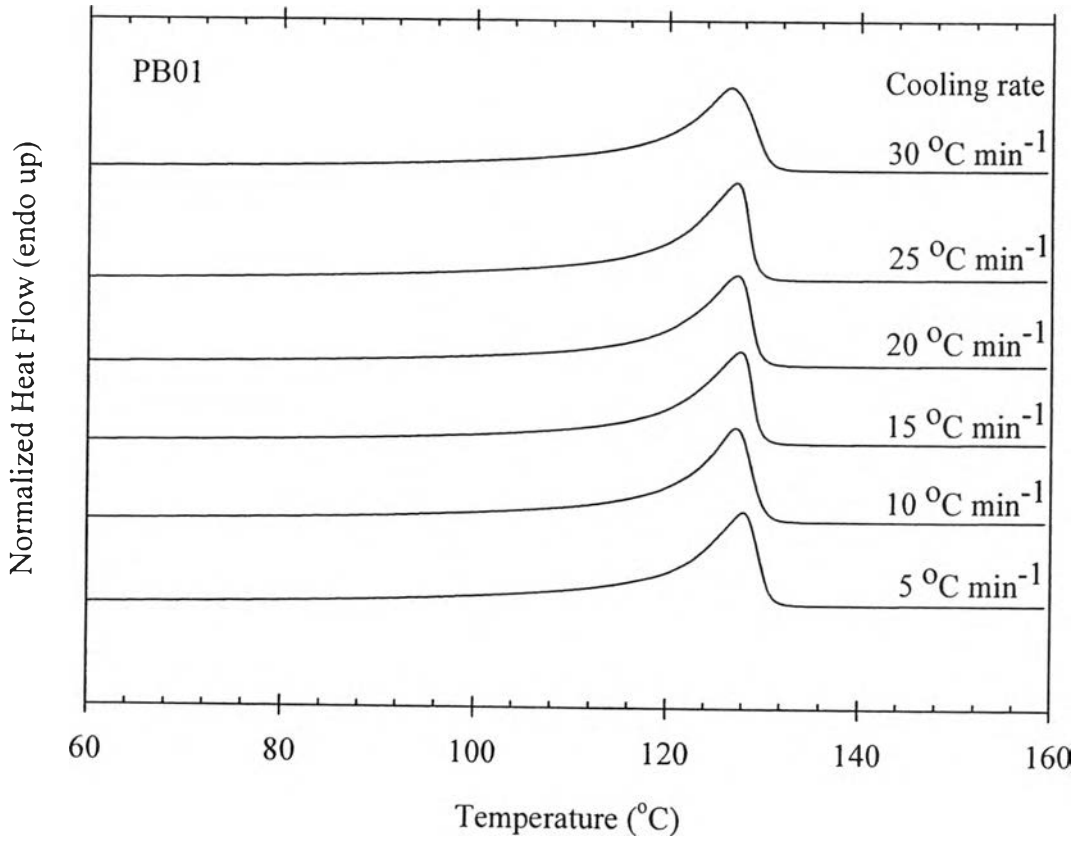

Figure 6.2(b) Corresponding subsequent melting endotherm recorded at a heating rate of 20°C min^{-1}

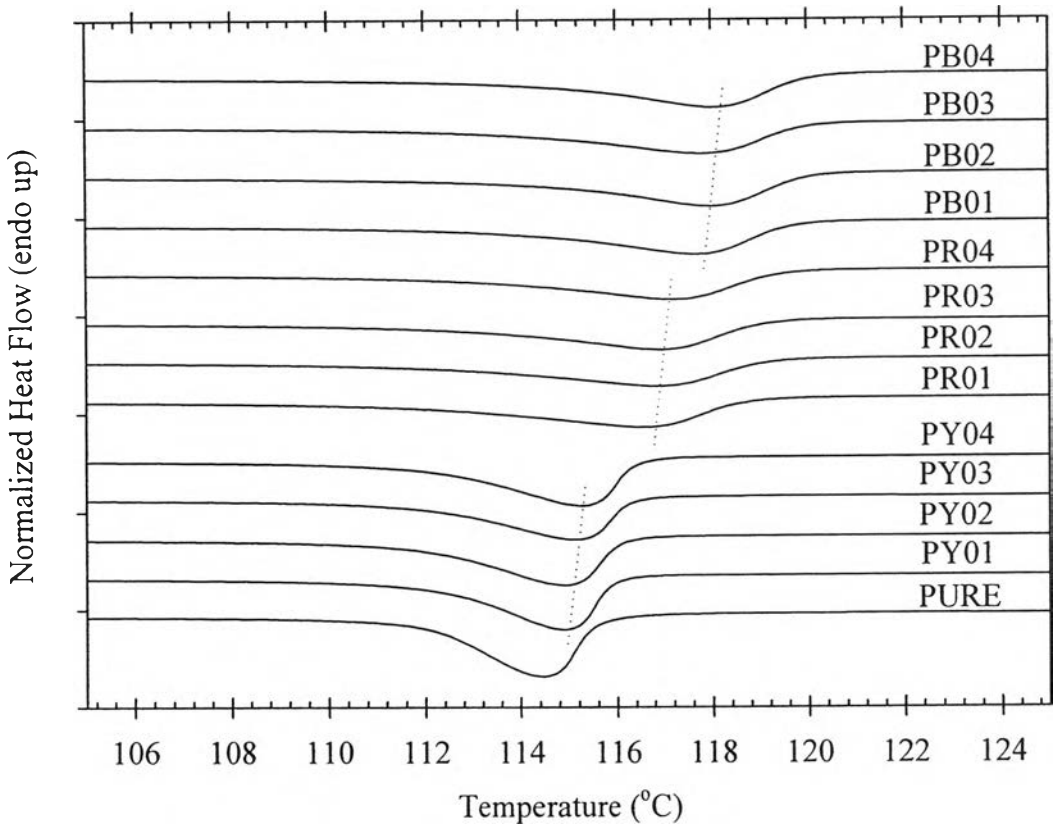

Figure 6.3(a) Non-isothermal melt-crystallzation exotherm of neat and pigmented MDPE recorded at a cooling rate of $10^{o}C\ min^{-1}$

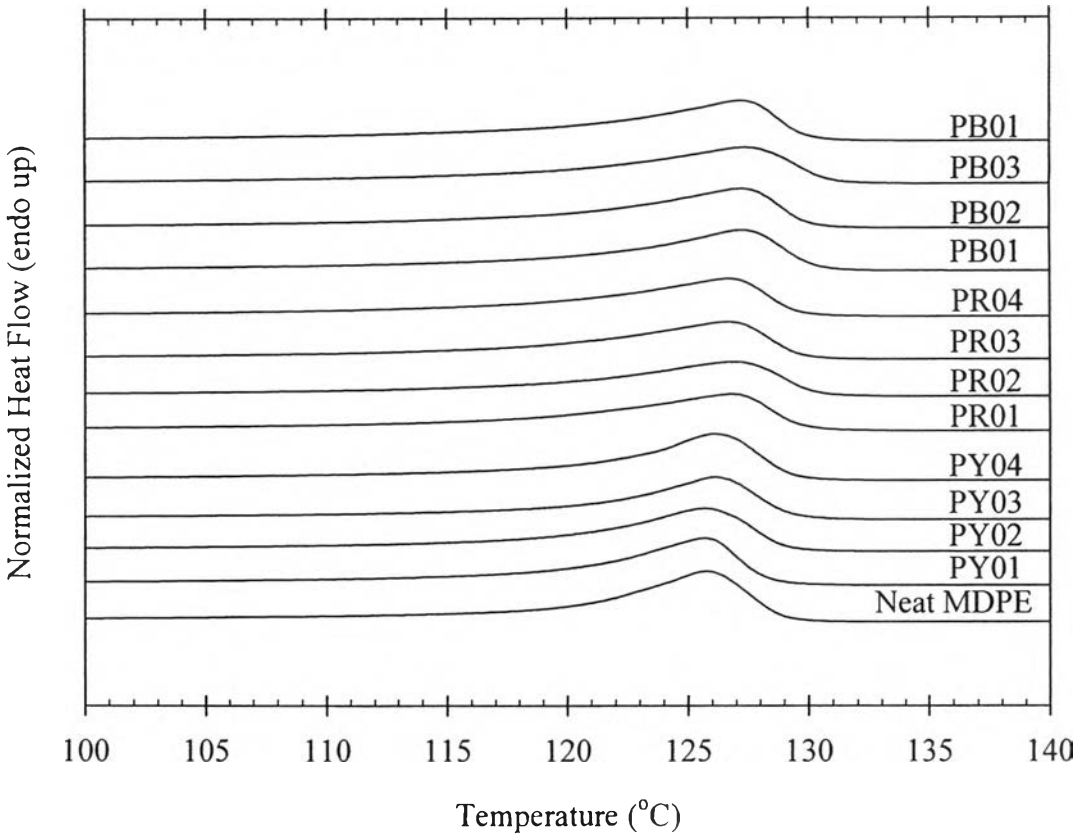

Figure 6.3(b) Corresponding subsequent melting endotherm recorded at a heating rate of 20°C min^{-1}.

Table 6.1 Characteristic data of non-isothermal melt-crystallization exotherms for neat MDPE and pigmented MDPE

ϕ (°C min^{-1})	$T_{0.01}$ (°C)	T_p (°C)	$T_{0.99}$ (°C)	$T_{0.01}$ (°C)	T_p (°C)	$T_{0.99}$ (°C)
	PY01			PY02		
5	117.6	116.6	114.6	117.9	117.0	114.6
10	116.0	114.8	111.8	116.2	114.9	111.3
15	116.3	115.9	109.9	116.6	115.5	111.2
20	116.1	114.5	108.0	116.2	115.0	109.0
25	115.6	113.6	107.7	115.8	114.1	107.9
30	115.4	113.6	106.1	115.8	113.7	105.7
	PY03			PY04		
5	118.0	117.0	114.5	118.1	117.1	114.8
10	116.3	115.2	111.3	116.5	115.3	111.6
15	116.8	115.4	110.0	116.8	115.4	110.0
20	116.3	114.4	108.4	116.5	115.1	108.9
25	116.0	114.1	106.1	116.1	114.4	106.5
30	115.8	114.0	105.1	115.9	114.2	105.7
	PB01			PB02		
5	120.8	119.0	115.9	121.1	119.4	116.0
10	119.7	117.8	112.7	120.1	118.0	113.4
15	119.4	116.5	111.1	119.7	116.7	111.3
20	119.0	115.6	108.5	119.3	116.0	109.1
25	118.7	115.9	107.3	119.1	115.4	107.2
30	118.7	114.6	103.5	119.2	115.8	104.3
	PB03			PB04		
5	121.0	119.3	116.2	121.1	119.2	115.8
10	120.0	117.8	112.4	120.1	118.1	113.5
15	119.8	117.0	111.9	119.2	117.0	112.0
20	119.4	116.3	110.3	119.2	115.7	108.3
25	119.1	115.8	108.6	119.0	115.4	108.6
30	119.2	116.2	107.1	119.3	115.7	105.1

Table 6.1 Characteristic data of non-isothermal melt-crystallization exotherms for neat MDPE and pigmented MDPE (*continued*)

ϕ (°C min^{-1})	$T_{0.01}$ (°C)	T_p (°C)	$T_{0.99}$ (°C)	$T_{0.01}$ (°C)	T_p (°C)	$T_{0.99}$ (°C)
	PR01			PR02		
5	120.6	118.9	115.0	120.9	119.0	115.4
10	118.8	116.6	110.7	119.2	117.0	111.0
15	119.0	116.0	109.3	119.4	116.5	110.3
20	118.9	116.1	107.7	119.2	116.5	108.8
25	118.5	115.8	106.3	118.9	115.5	106.7
30	118.4	115.4	105.4	118.9	115.4	104.4
	PR03			PR04		
5	121.0	119.0	115.0	121.2	119.2	115.5
10	119.2	116.9	111.6	119.5	117.2	111.8
15	119.4	116.5	110.6	119.6	116.5	110.1
20	119.1	116.4	108.8	119.4	116.5	107.5
25	119.0	116.0	107.5	119.2	116.0	106.8
30	118.8	115.6	106.0	119.1	115.8	105.9
	neat MDPE					
5	116.8	115.5	113.5			
10	115.6	114.5	111.6			
15	115.0	112.7	109.0			
20	114.5	111.7	107.5			
25	114.3	111.2	107.1			
30	114.5	112.2	105.1			

The data can be further analyzed by converting the non-isothermal crystallization exotherm to the relative crystallinity as a function of time $\theta(t)$ using Eq. (6.1) together with Eq. (6.2). The converted curves for PY01 at different cooling rates are illustrated in Fig. 6.4. According to Fig. 6.4, it is clear that the faster the cooling rate, the shorter the time required for the completion of the crystallization process. Other samples including neat MDPE samples exhibited a similar behavior.

It is worth noting that these $\theta(t)$ curves do not include the apparent incubation period Δt_{inc}, defined as a time period during which the polymer is still in the molten state (i.e. $\Delta t_{inc} = (T_f - T_{onset})/\phi$, where T_f is the fusion temperature or the temperature where a polymer sample is brought to melt, T_{onset} is the actual temperature where the sample begins to crystallize, and ϕ is the cooling rate). The Δt_{inc} values were calculated based on a T_f value of 160°C and the results are summarized in Table 6.2. For each sample, Dtinc decreased monotonically with increasing cooling rate.

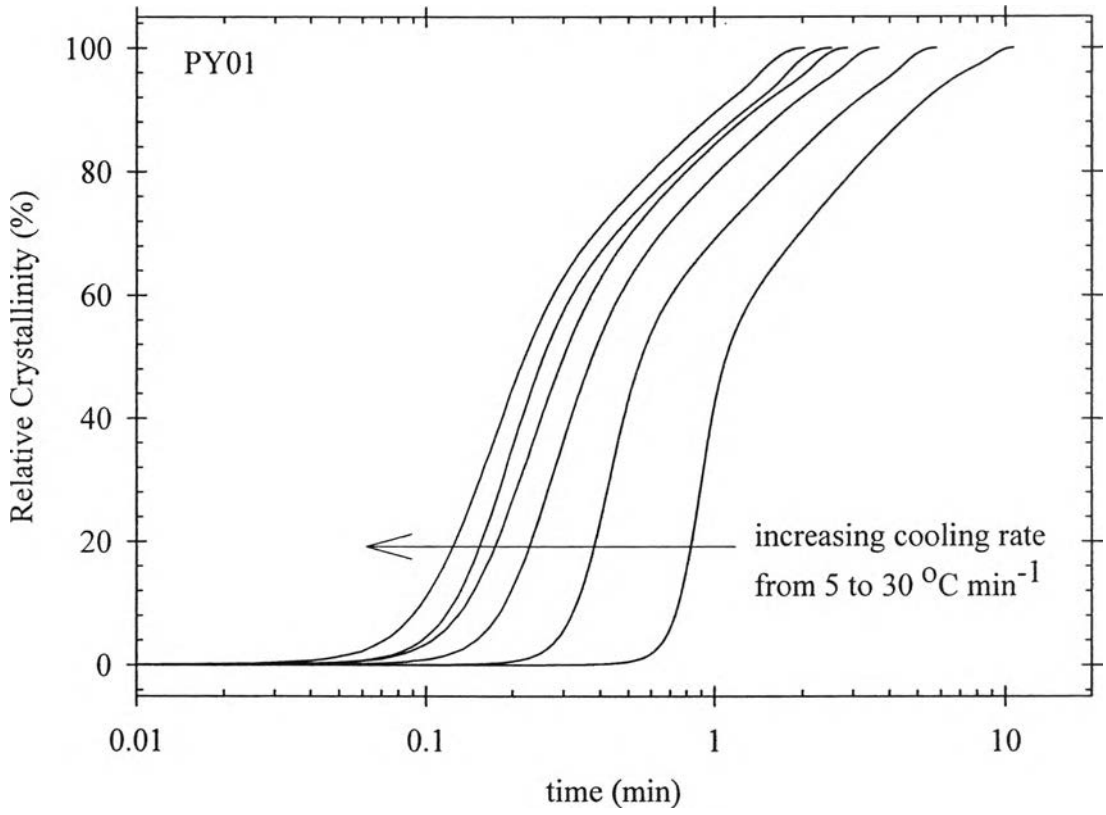

Figure 6.4 Relative crystallinity as a function of time of MDPE filled with 0.1 phr of diarylide (PY01) at six different cooling rates ranging from 5 to 30°C min^{-1}.

Table 6.2 Quantitative analysis of the relative crystallinity as a functions of time for neat MDPE

ϕ (°C min^{-1})	Δt_{inc} (min)	t_θ (min) θ= 0.01	θ= 0.1	θ= 0.3	θ= 0.5	θ= 0.7	θ= 0.9	θ= 0.99	Δt_c (min)
	Neat MDPE								
5	7.42	0.42	0.69	0.96	1.48	2.83	6.58	10.57	10.15
10	3.76	0.28	0.44	0.60	0.85	1.50	3.41	5.55	5.27
15	2.60	0.11	0.23	0.35	0.54	1.01	2.42	3.80	3.69
20	1.97	0.09	0.19	0.29	0.43	0.77	1.81	2.86	2.77
25	1.60	0.06	0.14	0.23	0.34	0.58	1.36	2.18	2.11
30	1.34	0.06	0.13	0.22	0.32	0.50	1.13	1.84	1.78

Furthermore, the crystallization time at an arbitrary relative crystallinity t_θ can be determined from the $\theta(t)$ curves. The t_θ values after exclusion of the respective Δt_{inc} values for various relative crystallinity values (i.e. θ = 0.01, 0.1, 0.3, 0.5, 0.7, 0.9, and 0.99) for all of the samples investigated are summarized in Tables 6.2–6.5, while Fig. 6.5 shows plots of tq as a function of cooling rate for PR01. The apparent total crystallization period Δt_c can be calculated directly from the difference between the apparent ending and the apparent onset of the crystallization process in the time domain (i.e. $\Delta t_c = t_{0.99} - t_{0.01}$). These values for all of the samples investigated are also summarized in Tables 6.2–6.5.

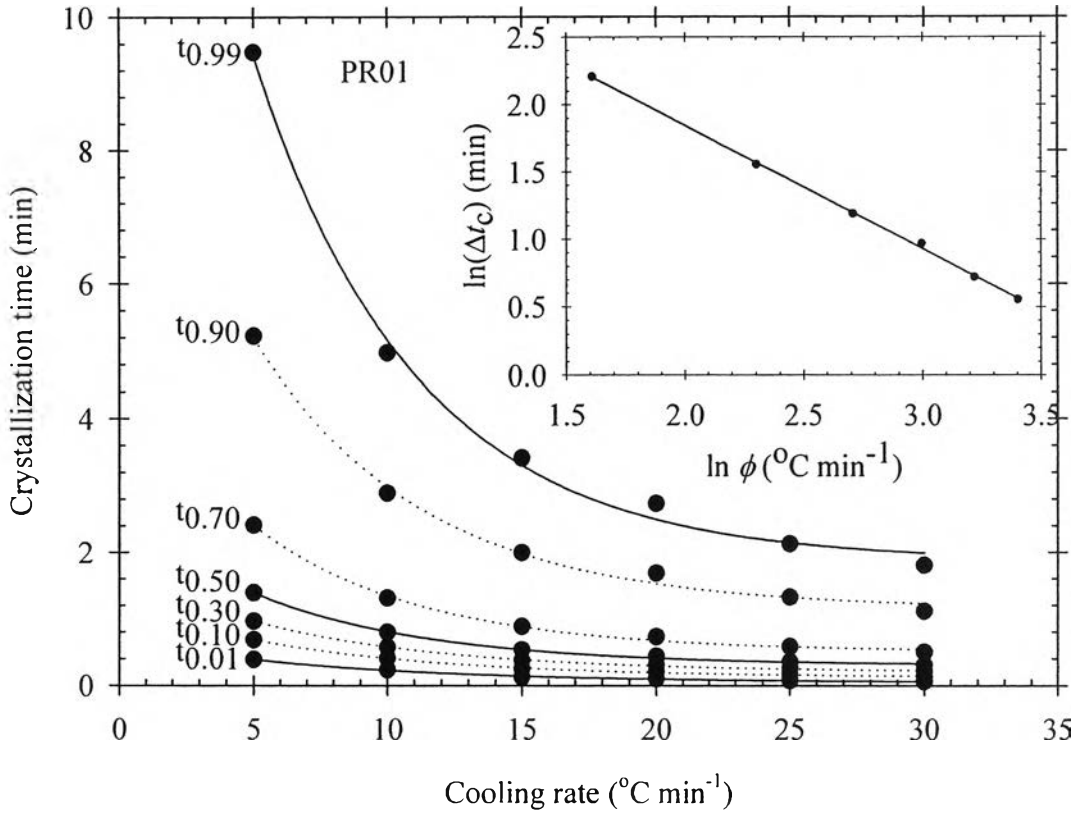

Figure 6.5 Crystallization time at various relative crystallinity values as a function of cooling rate for MDPE filled with 0.1 phr of quinacridone (PR01). The inset figure shows a relationship between apparent total crystallization period and cooling rate in a log-log plot.

Table 6.3 Quantitative analysis of the relative crystallinity as a functions of time for MDPE filled with various amount of diarylide

ϕ (°C min^{-1})	Δt_{inc} (min)	t_θ (min)							Δt_c (min)
		θ= 0.01	θ= 0.1	θ= 0.3	θ= 0.5	θ= 0.7	θ= 0.9	θ= 0.99	
	PY01								
5	7.94	0.51	0.70	0.86	1.05	1.90	4.81	9.22	8.71
10	4.18	0.22	0.33	0.43	0.56	1.04	2.83	4.95	4.73
15	2.82	0.10	0.19	0.27	0.38	0.65	1.75	3.16	3.05
20	2.15	0.07	0.14	0.21	0.30	0.51	1.38	2.45	2.38
25	1.73	0.06	0.12	0.18	0.26	0.45	1.28	2.11	2.05
30	1.46	0.05	0.10	0.15	0.22	0.38	1.03	1.71	1.66
	PY02								
5	8.08	0.31	0.51	0.68	0.92	1.89	5.24	9.58	9.27
10	4.19	0.20	0.31	0.42	0.57	1.08	2.93	5.05	4.85
15	2.81	0.10	0.18	0.25	0.35	0.66	1.77	3.18	3.08
20	2.14	0.07	0.14	0.21	0.29	0.54	1.52	2.56	2.48
25	1.74	0.05	0.10	0.16	0.23	0.39	1.06	1.92	1.88
30	1.45	0.04	0.10	0.15	0.22	0.36	0.89	1.61	1.57
	PY03								
5	7.78	0.59	0.80	0.98	1.25	2.33	5.84	10.15	9.56
10	4.19	0.19	0.31	0.42	0.56	1.02	2.56	4.75	4.56
15	2.80	0.10	0.19	0.28	0.39	0.71	1.85	3.27	3.17
20	2.13	0.07	0.15	0.22	0.32	0.56	1.51	2.57	2.49
25	1.73	0.05	0.12	0.19	0.27	0.45	1.12	1.98	1.93
30	1.46	0.04	0.10	0.16	0.23	0.39	0.97	1.68	1.64
	PY04								
5	8.10	0.25	0.45	0.60	0.78	1.35	3.24	5.93	5.68
10	4.19	0.16	0.28	0.38	0.52	0.94	2.43	4.56	4.40
15	2.79	0.10	0.19	0.28	0.39	0.69	1.82	3.24	3.14
20	2.12	0.07	0.15	0.22	0.31	0.57	1.55	2.60	2.53
25	1.72	0.06	0.12	0.19	0.27	0.46	1.22	2.05	1.99
30	1.45	0.04	0.09	0.15	0.22	0.36	0.89	1.62	1.58

Table 6.4 Quantitative analysis of the relative crystallinity as a functions of time for MDPE filled with various amount of phthalocyanine

ϕ (°C min^{-1})	Δt_{inc}	t_θ (min)							Δt_c
	(min)	θ= 0.01	θ= 0.1	θ= 0.3	θ= 0.5	θ= 0.7	θ= 0.9	θ= 0.99	(min)
	PB01								
5	7.42	0.42	0.69	0.96	1.48	2.83	6.58	10.57	10.15
10	3.76	0.28	0.44	0.60	0.85	1.50	3.41	5.55	5.27
15	2.60	0.11	0.23	0.35	0.54	1.01	2.42	3.80	3.69
20	1.97	0.09	0.19	0.29	0.43	0.77	1.81	2.86	2.77
25	1.60	0.06	0.14	0.23	0.34	0.58	1.36	2.18	2.11
30	1.34	0.06	0.13	0.22	0.32	0.50	1.13	1.84	1.78
	PB02								
5	7.38	0.42	0.68	0.95	1.44	2.64	5.89	10.19	9.77
10	3.75	0.26	0.41	0.57	0.82	1.46	3.20	5.30	5.04
15	2.56	0.13	0.25	0.37	0.55	1.00	2.28	3.63	3.50
20	1.95	0.10	0.19	0.30	0.44	0.80	1.91	3.05	2.95
25	1.58	0.07	0.14	0.24	0.35	0.60	1.34	2.17	2.10
30	1.33	0.05	0.13	0.21	0.31	0.50	1.11	1.80	1.75
	PB03								
5	7.25	0.55	0.81	1.07	1.54	2.70	5.85	10.16	9.61
10	3.74	0.28	0.44	0.61	0.86	1.47	3.23	5.35	5.07
15	2.57	0.12	0.23	0.35	0.53	1.00	2.38	3.61	3.49
20	1.96	0.08	0.17	0.27	0.42	0.81	1.92	2.83	2.75
25	1.57	0.07	0.15	0.23	0.35	0.62	1.46	2.29	2.22
30	1.32	0.06	0.13	0.20	0.30	0.51	1.18	1.80	1.75
	PB04								
5	6.77	1.03	1.32	1.62	2.22	3.77	8.00	12.48	11.45
10	3.78	0.23	0.38	0.54	0.78	1.38	3.06	5.09	4.87
15	2.59	0.10	0.22	0.34	0.51	0.97	2.24	3.60	3.50
20	1.96	0.08	0.18	0.29	0.42	0.72	1.66	2.71	2.63
25	1.57	0.07	0.15	0.23	0.34	0.60	1.40	2.17	2.09
30	1.32	0.06	0.13	0.22	0.33	0.56	1.23	1.91	1.85

Table 6.5 Quantitative analysis of the relative crystallinity as a functions of time for MDPE filled with various amount of quinacridone

ϕ (°C min^{-1})	Δt_{inc} (min)	t_θ (min)							Δt_c (min)
		θ= 0.01	θ= 0.1	θ= 0.3	θ= 0.5	θ= 0.7	θ= 0.9	θ= 0.99	
	PR01								
5	7.47	0.39	0.68	0.96	1.39	2.41	5.22	9.47	9.09
10	3.89	0.23	0.40	0.57	0.79	1.31	2.89	4.97	4.74
15	2.60	0.13	0.25	0.38	0.53	0.88	1.99	3.41	3.29
20	1.97	0.10	0.20	0.31	0.44	0.73	1.68	2.73	2.63
25	1.60	0.07	0.16	0.25	0.35	0.58	1.33	2.13	2.06
30	1.35	0.06	0.13	0.21	0.30	0.50	1.11	1.80	1.74
	PR02								
5	7.35	0.45	0.74	0.99	1.36	2.13	4.08	6.74	6.29
10	3.87	0.22	0.38	0.55	0.78	1.28	2.77	4.86	4.65
15	2.59	0.12	0.24	0.36	0.52	0.89	2.01	3.38	3.26
20	1.97	0.08	0.18	0.28	0.40	0.66	1.50	2.51	2.42
25	1.59	0.07	0.15	0.24	0.35	0.56	1.30	2.14	2.07
30	1.34	0.06	0.14	0.22	0.32	0.51	1.11	1.80	1.74
	PR03								
5	7.50	0.30	0.59	0.88	1.28	2.16	4.43	8.17	7.87
10	3.89	0.20	0.36	0.53	0.76	1.30	2.89	5.04	4.84
15	2.58	0.12	0.25	0.37	0.53	0.93	2.10	3.50	3.37
20	1.97	0.09	0.19	0.29	0.42	0.73	1.69	2.67	2.58
25	1.59	0.07	0.15	0.24	0.35	0.58	1.34	2.11	2.04
30	1.33	0.06	0.13	0.21	0.30	0.49	1.09	1.79	1.74
	PR04								
5	7.30	0.46	0.75	1.04	1.48	2.47	5.06	9.17	8.71
10	3.88	0.19	0.35	0.53	0.78	1.36	3.08	5.17	4.99
15	2.53	0.17	0.29	0.42	0.60	1.00	2.26	3.67	3.50
20	1.96	0.09	0.19	0.30	0.43	0.70	1.46	2.52	2.43
25	1.58	0.07	0.16	0.25	0.37	0.62	1.33	2.15	2.08
30	1.33	0.06	0.14	0.22	0.31	0.51	1.15	1.82	1.76

Table 6.6 y-intercept, slope, and the r^2 values of regression lines drawn through plots of $\ln(t_\theta)$ against $\ln(\phi)$ for various θ values

θ	y-intercept (min)	slope ($min^2\ ^oC^{-1}$)	r^2	y-intercept (min)	slope ($min^2\ ^oC^{-1}$)	r^2
	Neat MDPE					
0.01	1.204	-1.20	0.9624			
0.1	1.257	-0.98	0.9800			
0.3	1.397	-0.87	0.9854			
0.5	1.842	-0.89	0.9936			
0.7	2.636	-0.98	0.9982			
0.9	3.476	-0.97	0.9969			
0.99	3.953	-0.98	0.9985			
Δt_c	3.893	-0.97	0.9984			
	PY01			PY02		
0.01	1.512	-1.36	0.9870	0.841	-1.17	0.9761
0.1	1.428	-1.11	0.9927	0.977	-0.99	0.9863
0.3	1.373	-0.96	0.9962	1.053	-0.88	0.9871
0.5	1.431	-0.87	0.9976	1.277	-0.84	0.9880
0.7	2.095	-0.91	0.9940	2.214	-0.96	0.9927
0.9	2.972	-0.87	0.9908	3.295	-0.99	0.9908
0.99	3.736	-0.94	0.9977	3.882	-1.00	0.9980
Δt_c	3.653	-0.92	0.9981	3.837	-0.99	0.9982
	PY03			PY04		
0.01	1.730	-1.45	0.9936	0.421	-1.04	0.9697
0.1	1.572	-1.16	0.9909	0.668	-0.87	0.9909
0.3	1.503	-1.00	0.9881	0.75	-0.76	0.9946
0.5	1.627	-0.92	0.9882	0.908	-0.69	0.9928
0.7	2.383	-0.99	0.9936	1.514	-0.71	0.9782
0.9	3.288	-0.98	0.9923	2.375	-0.68	0.9414
0.99	3.890	-0.99	0.9983	3.058	-0.72	0.9559
Δt_c	3.803	-0.97	0.9985	2.998	-0.71	0.9545

Table 6.6 y-intercept, slope, and the r^2 values of regression lines drawn through plots of $\ln(t_\theta)$ against $\ln(\phi)$ for various θ values (*continued*)

θ	y-intercept (min)	slope ($min^2\ °C^{-1}$)	r^2	y-intercept (min)	slope ($min^2\ °C^{-1}$)	r^2
	PB01			PB02		
0.01	1.204	-1.20	0.9624	1.188	-1.19	0.9746
0.1	1.257	-0.98	0.9800	1.226	-0.96	0.9906
0.3	1.397	-0.87	0.9854	1.362	-0.86	0.9954
0.5	1.842	-0.89	0.9936	1.767	-0.87	0.9981
0.7	2.636	-0.98	0.9982	2.482	-0.92	0.9967
0.9	3.476	-0.97	0.9969	3.269	-0.91	0.9894
0.99	3.953	-0.98	0.9985	3.866	-0.95	0.9937
Δt_c	3.893	-0.97	0.9984	3.804	-0.94	0.9935
	PB03			PB04		
0.01	1.624	-1.35	0.9790	2.353	-1.590	0.9559
0.1	1.554	-1.08	0.9873	2.117	-1.265	0.9589
0.3	1.642	-0.97	0.9904	2.099	-1.111	0.9583
0.5	1.946	-0.93	0.9963	2.366	-1.069	0.9652
0.7	2.491	-0.92	0.9972	2.925	-1.069	0.9773
0.9	3.188	-0.87	0.9932	3.631	-1.030	0.9827
0.99	3.854	-0.95	0.9985	4.128	-1.042	0.9916
Δt_c	3.769	-0.93	0.9981	4.005	-1.012	0.9932
	PR01			PR02		
0.01	0.850	-1.07	0.9851	1.096	-1.17	0.9962
0.1	1.135	-0.92	0.9951	1.237	-0.97	0.9959
0.3	1.348	-0.85	0.9976	1.380	-0.87	0.9941
0.5	1.705	-0.85	0.9988	1.652	-0.84	0.9948
0.7	2.292	-0.88	0.9989	2.105	-0.83	0.9964
0.9	3.022	-0.85	0.9978	2.654	-0.74	0.9895
0.99	3.730	-0.92	0.9992	3.216	-0.76	0.9794
Δtc	3.675	-0.91	0.9992	3.119	-0.74	0.9757

Table 6.6 y-intercept, slope, and the r^2 values of regression lines drawn through plots of $\ln(t_\theta)$ against $\ln(\phi)$ for various θ values (*continued*)

θ	y-intercept (min)	slope ($min^2\ °C^{-1}$)	r^2	y-intercept (min)	slope ($min^2\ °C^{-1}$)	r^2
	PR03			PR04		
0.01	0.395	-0.93	0.9844	1.040	-1.130	0.9742
0.1	0.898	-0.86	0.9961	1.234	-0.954	0.9896
0.3	1.196	-0.81	0.9986	1.425	-0.872	0.9945
0.5	1.576	-0.82	0.9992	1.776	-0.866	0.9972
0.7	2.137	-0.83	0.9963	2.336	-0.882	0.9961
0.9	2.789	-0.77	0.9882	3.046	-0.857	0.9853
0.99	3.529	-0.86	0.9939	3.724	-0.918	0.9954
Δt_c	3.486	-0.85	0.9942	3.659	-0.908	0.9955

According to the data presented in these tables, the t_θ value for a given value of θ and the Δt_c value were all found to decrease with increasing cooling rate, indicating that non-isothermal melt-crystallization proceeds faster with increasing cooling rate. In an attempt to further analyze the results shown in these tables, plots of $\ln(\Delta t_c)$ versus $\ln(\phi)$ (shown as the inset in Fig. 6.5 for PR01) and of $\ln(t_\theta)$ versus $\ln(\phi)$ (shown in Fig. 6.6 for PR01) were carried out. Interestingly, the linearity of these plots is evident. Table 6.6 summarizes values of the y-intercept and the slope obtained from these plots for all of the samples investigated. Interestingly, for a given sample type, the y-intercept of these plots was found to increase with increasing θ, while the slope was found to be essentially similar.

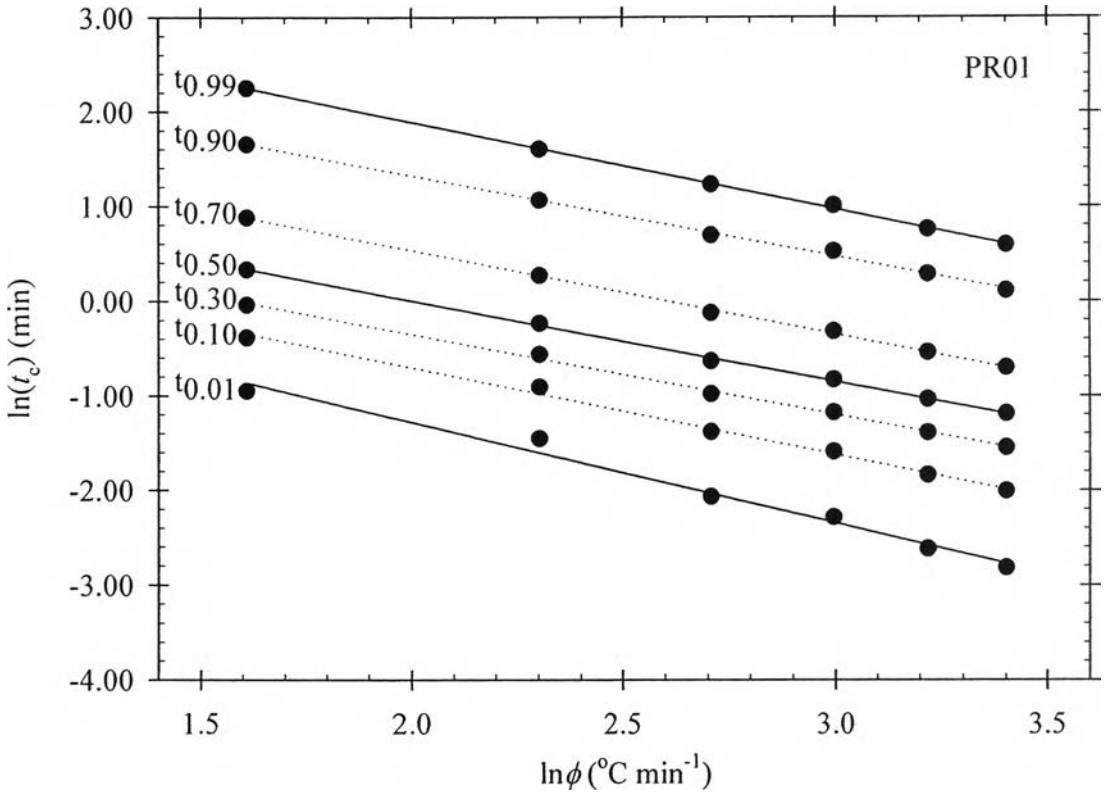

Figure 6.6 Crystallization time at various relative crystallinity values as a function of cooling rate in a log-log plot for MDPE filled with 0.1 phr of quinacridone (PR01).

As previously mentioned, subsequent melting endotherms of neat and pigmented MDPE samples which were non-isothermally crystallized at a rate of 10°C min^{-1} are shown in Fig. 6.3. Apparently, only one melting endotherm was observed in these thermograms. The single melting endotherm was also observed for samples which were non-isothermally crystallized at different cooling rates. The apparent melting temperature T_m and the apparent enthalpy of fusion ΔH_f of these samples observed at different cooling rates are summarized in Table 6.7. Obviously, no significant difference in the T_m value for all of the samples investigated was observed.

On the other hand, for a given sample type, the observed ΔH_f value was found to be a decreasing function of the cooling rate used, indicating that the apparent degree of the crystallinity was also a decreasing function of the cooling rate.

Table 6.7 Characteristic data of subsequent melting endotherms after non-isothermal melt-crystallization for neat and pigmented MDPE

ϕ (°C min^{-1})	T_m (°C)	ΔH_f (Jg^{-1})	T_m (°C)	ΔH_f (Jg^{-1})	T_m (°C)	ΔH_f (Jg^{-1})	T_m (°C)	ΔH_f (Jg^{-1})
	PY01		PY02		PY03		PY04	
5	126.9	165.2	127.2	151.4	126.9	149.5	127.1	155.5
10	125.7	150.1	125.8	152.0	126.0	140.5	126.0	153.5
15	126.2	131.8	126.5	149.2	126.7	144.9	126.3	144.6
20	125.9	140.9	126.1	153.2	126.2	149.5	127.0	147.6
25	125.6	151.6	125.6	142.5	126.0	142.3	126.3	147.0
30	126.1	147.3	126.0	139.8	125.8	144.9	125.7	136.7
	PB01		PB02		PB03		PB04	
5	127.9	158.9	128.0	154.5	128.0	155.1	128.5	153.2
10	127.1	155.7	127.2	151.8	127.4	152.8	127.1	155.3
15	127.8	151.8	127.8	154.6	127.8	153.8	127.9	146.6
20	127.1	154.8	126.1	149.8	127.2	147.6	127.5	152.1
25	127.1	153.5	127.1	147.9	127.1	151.7	156.8	146.5
30	126.6	157.8	126.8	153.0	126.5	144.0	126.5	147.8
	PR01		PR02		PR03		PR04	
5	128.8	153.1	128.3	154.4	128.2	153.2	128.2	162.9
10	126.8	149.3	127.0	141.3	126.7	151.5	126.5	151.9
15	128.5	150.5	127.5	151.1	127.5	151.6	127.8	146.9
20	127.0	149.0	126.6	153.0	126.9	150.1	126.9	148.5
25	126.4	144.9	126.6	153.0	126.3	153.2	126.5	149.1
30	126.0	145.6	126.3	146.1	126.0	143.7	126.1	144.0
	Neat MDPE							
5	126.4	154.8						
10	125.8	158.7						
15	126.5	153.8						
20	126.8	148.2						
25	126.1	158.9						
30	125.4	151.5						

6.5.2 Non-Isothermal Melt-Crystallization Based on Avrami Analysis

According to Fig. 6.4, each $\theta(t)$ curve exhibited two regions, which should correspond to the primary and secondary crystallization processes. Primary crystallization occurs during the early stage of crystallization and is thought to end as soon as adjacent spherulites or other forms of crystalline aggregates impinge upon one another. Secondary crystallization involves thickening of the crystals, growth of new lamellae within or between existing lamellar stacks, and growth of new lamellar stacks from the remaining amorphous regions (but crystallizable) within the spherulites. During the secondary crystallization, a refinement of existing crystals through the removal of lattice defect distortions is also possible [14]. In this work, the primary crystallization was thought to cover the θ range of 0.1–0.4, while the secondary crystallization was thought to cover the θ range of 0.6–0.9. Each of the two regions was subsequently analyzed according to the Avrami model [7–9].

In an attempt to analyze the non-isothermal melt-crystallization data based on the Avrami model, Eq. (6.3) can be arranged to the following form:

$$\ln[-\ln(1-\theta(t))] = n_A \ln K_A + n_A \ln t . \tag{6.4}$$

Based on this equation, the Avrami kinetic parameters (i.e. K_A and n_A) could be obtained from a plot between $\ln[-\ln(1-\theta(t))]$ and $\ln t$, as shown in Fig. 6.7 for PY01. Tables 6.8 and 6.9 summarize values of the Avrami kinetic parameters for all of the samples analyzed along with the values of the r^2 parameter signifying the quality of the fitting during both primary and secondary crystallization processes. Based on the values of the r^2 parameter, it can be concluded that the Avrami model was suitable for describing non-isothermal melt-crystallization data of these samples. It should be noted that subscripts '1' and '2' were used to denote the Avrami kinetic parameters obtained for the primary and the secondary crystallization processes, respectively.

According to the values reported in Tables 6.8 and 6.9, the Avrami rate constants for both primary and secondary crystallization processes (i.e. K_{A1} and K_{A2},

respectively) increased with increasing cooling rate. Among the various pigments investigated, diarylide was the best in accelerating crystallization processes of the corresponding pigmented MDPE samples (PY), despite the fact that phthalocyanine was the best in shifting the crystallization range to a higher temperature range. For pure MDPE, the Avrami exponent specific to the primary crystallization process was found to range between 3.0 and 6.9, while, for all of the pigmented samples, it was found to range between 2.2 and 6.3. Interestingly, the Avrami exponent specific to the secondary crystallization process exhibited a value, a little lower than 1.0. Specifically, it was found to range around 0.6 and 0.7 for pure MDPE, and between 0.6 and 1.0 for all of the pigmented samples.

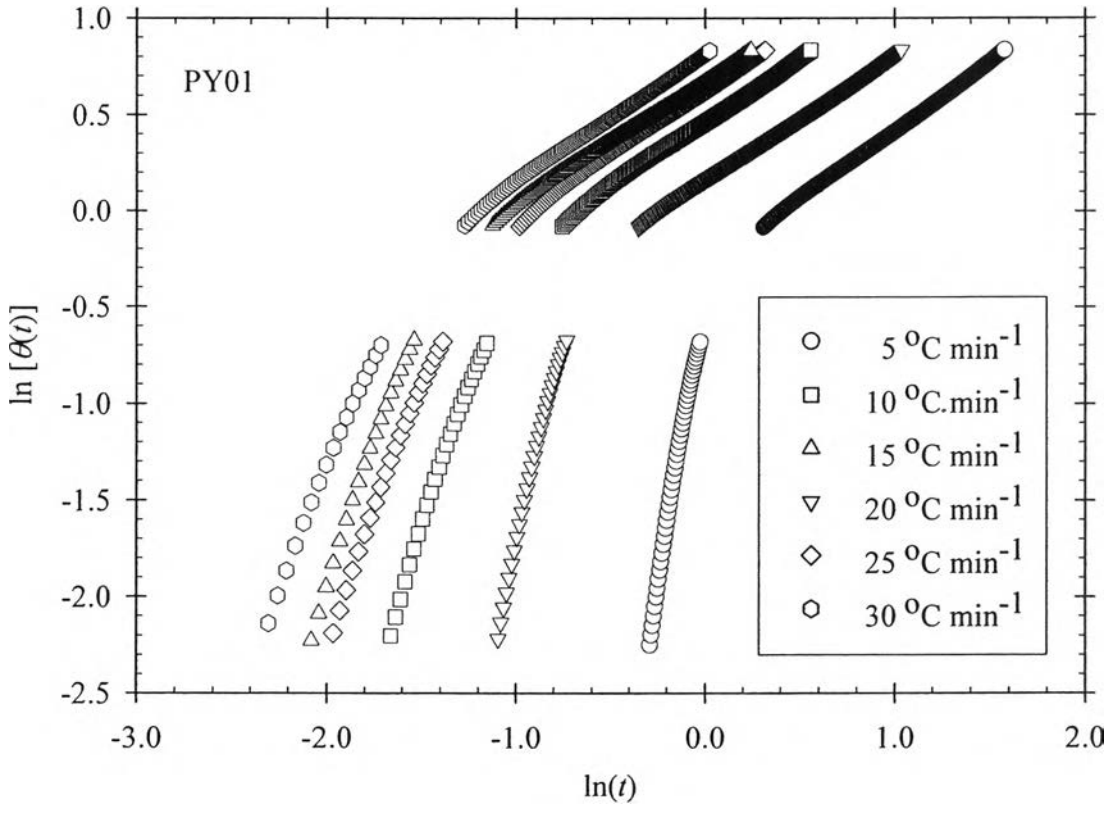

Figure 6.7 Typical Avrami analysis for MDPE filled with 0.1 phr of diarylide (PY01).

Table 6.8 Non-isothermal melt-crystallization kinetics for pure MDPE and pigment-added MDPE based on Avrami analysis for primary crystallization process (covering the θ range of 0.1-0.4)

ϕ (°C min^{-1})	K_{A1} (min^{-1})	n_{A1}	r^2	K_{A1} (min^{-1})	n_{A1}	r^2
	Neat MDPE					
5	0.78	6.9	0.9976			
10	1.46	6.4	0.9971			
15	1.93	5.0	0.9920			
20	2.64	4.3	0.9955			
25	4.03	3.0	0.9970			
30	3.85	3.1	0.9965			
	PY01			PY02		
5	0.93	6.0	0.9919	1.12	3.9	0.9915
10	1.82	4.3	0.9917	1.78	3.7	0.9907
15	2.58	3.0	0.9934	2.83	3.1	0.9929
20	3.14	2.6	0.9945	3.29	2.7	0.9937
25	3.76	2.8	0.9933	4.13	2.6	0.9950
30	4.26	2.4	0.9956	4.20	2.4	0.9964
	PY03			PY04		
5	0.80	5.7	0.9858	1.264	3.9	0.9952
10	1.78	3.6	0.9919	1.904	3.4	0.9921
15	2.49	2.8	0.9934	2.478	2.8	0.9930
20	3.03	2.7	0.9938	3.068	2.7	0.9932
25	3.42	2.4	0.9955	3.433	2.4	0.9948
30	3.97	2.3	0.9962	4.158	2.3	0.9967

Table 6.8 Non-isothermal melt-crystallization kinetics for pure MDPE and pigment-added MDPE based on Avrami analysis for primary crystallization process (covering the θ range of 0.1-0.4) (*continued*)

ϕ (°C min^{-1})	K_{AI} (min^{-1})	n_{AI}	r^2	K_{AI} (min^{-1})	n_{AI}	r^2
	PB01			PB02		
5	0.79	3.7	0.9935	0.79	3.6	0.9946
10	1.26	3.6	0.9914	1.29	3.5	0.9904
15	1.85	2.5	0.9899	1.81	2.6	0.9900
20	2.25	2.5	0.9927	2.19	2.5	0.9913
25	2.81	2.4	0.9942	2.69	2.3	0.9943
30	2.86	2.3	0.9966	2.93	2.2	0.9968
	PB03			PB04		
5	0.69	4.2	0.9873	0.486	6.3	0.9874
10	1.21	3.4	0.9914	1.359	3.3	0.9918
15	1.95	2.7	0.9929	1.939	2.5	0.9902
20	2.35	2.3	0.9906	2.252	2.4	0.9939
25	2.79	2.5	0.9923	2.801	2.5	0.9929
30	3.18	2.4	0.9947	2.851	2.3	0.9949
	PR01			PR02		
5	0.78	3.5	0.9944	0.74	3.5	0.9879
10	1.25	3.1	0.9892	1.26	3.0	0.9901
15	1.81	2.7	0.9929	1.85	2.7	0.9920
20	2.18	2.7	0.9933	2.39	2.6	0.9938
25	2.65	2.5	0.9949	2.72	2.5	0.9954
30	3.08	2.5	0.9957	2.90	2.3	0.9964
	PR03			PR04		
5	0.78	2.8	0.9897	0.691	3.2	0.9843
10	1.31	2.9	0.9893	1.279	2.7	0.9887
15	1.84	2.7	0.9911	1.653	2.9	0.9895
20	2.29	2.6	0.9926	2.197	2.5	0.9944
25	2.74	2.5	0.9941	2.572	2.4	0.9940
30	3.14	2.5	0.9952	3.019	2.4	0.9952

Table 6.9 Non-isothermal melt-crystallization kinetics for pure MDPE and pigment-added MDPE based on Avrami analysis for secondary crystallization process (covering the θ range of 0.6-0.9)

ϕ (°C min^{-1})	K_{AI} (min^{-1})	n_{AI}	r^2	K_{AI} (min^{-1})	n_{AI}	r^2
	Neat MDPE					
5	0.61	0.6	0.9979			
10	1.26	0.7	0.9988			
15	1.59	0.7	0.9989			
20	2.37	0.7	0.9955			
25	3.36	0.6	0.9979			
30	3.50	0.7	0.9941			
	PY01			PY02		
5	0.66	0.7	0.9996	0.71	0.6	0.9994
10	1.27	0.6	0.9996	1.22	0.6	0.9996
15	2.01	0.7	0.9988	2.01	0.6	0.9991
20	2.57	0.7	0.998	2.46	0.6	0.9992
25	2.93	0.6	0.9988	3.37	0.7	0.9981
30	3.41	0.7	0.9986	3.55	0.7	0.9971
	PY03			PY04		
5	0.54	0.7	0.9997	0.95	0.7	0.9994
10	1.27	0.7	0.9992	1.38	0.7	0.9995
15	1.84	0.7	0.9994	1.87	0.7	0.9993
20	2.34	0.7	0.999	2.30	0.7	0.9993
25	2.85	0.7	0.9979	2.80	0.7	0.9981
30	3.32	0.7	0.9971	3.48	0.7	0.998

Table 6.9 Non-isothermal melt-crystallization kinetics for pure MDPE and pigment-added MDPE based on Avrami analysis for secondary crystallization process (covering the θ range of 0.6-0.9) (*continued*)

ϕ (°C min^{-1})	K_{A1} (min^{-1})	n_{A1}	r^2	K_{A1} (min^{-1})	n_{A1}	r^2
	PB01			PB02		
5	0.45	0.8	0.9998	0.47	0.8	0.9999
10	0.84	0.8	0.9998	0.86	0.8	0.9999
15	1.26	0.7	0.9995	1.27	0.8	0.9998
20	1.65	0.8	0.9997	1.60	0.7	0.9997
25	2.19	0.8	0.9993	2.08	0.8	0.9995
30	2.49	0.8	0.9964	2.48	0.8	0.9974
	PB03			PB04		
5	0.45	0.9	0.9998	0.31	0.9	0.9997
10	0.84	0.8	0.9997	0.90	0.8	0.9999
15	1.29	0.7	0.9997	1.31	0.8	0.9997
20	1.58	0.7	0.9988	1.75	0.8	0.9992
25	2.04	0.8	0.9997	2.10	0.8	0.9995
30	2.47	0.8	0.9994	2.22	0.8	0.9994
	PR01			PR02		
5	0.51	0.8	0.9998	0.56	1.0	0.9997
10	0.95	0.8	0.9994	0.97	0.8	0.9993
15	1.42	0.8	0.9993	1.40	0.8	0.9996
20	1.73	0.8	0.999	1.88	0.8	0.9992
25	2.15	0.8	0.9988	2.23	0.8	0.9984
30	2.51	0.8	0.999	2.43	0.8	0.9986
	PR03			PR04		
5	0.57	0.9	0.9998	0.49	0.9	0.9998
10	0.96	0.8	0.9996	0.92	0.8	0.9997
15	1.35	0.8	0.9998	1.25	0.8	0.9993
20	1.73	0.8	0.9995	1.76	0.9	0.9995
25	2.14	0.8	0.9993	2.00	0.9	0.9998
30	2.56	0.8	0.9986	2.43	0.8	0.9991

6.6 Conclusions

Non-isothermal melt-crystallization and subsequent melting behavior of neat MDPE and MDPE filled with three types of pigments (i.e. quinacridone, phthalocyanine, and diarylide) in various amounts ranging between 0.1 and 0.4 phr were investigated using differential scanning calorimetry. For each type of sample investigated, the crystallization exotherm became wider and shifted towards a lower temperature range when the cooling rate increased. All of the pigments investigated were able to shift the crystallization exotherm towards a higher temperature range, indicating that these pigments promoted the formation of heterogeneous nuclei. Among the various pigments, phthalocyanine was the best in shifting the crystallization exotherm towards a higher temperature range, followed by quinacridone and diarylide, respectively. However, diarylide was the only pigment that was effective in accelerating the crystallization processes of the filled polymer.

6.7 Acknowledgements

This work was supported in parts by the Thailand Research Fund (TRF) through the Royal Golden Jubilee PhD Program (2.L.CU/45/H.1), the Petroleum and Petrochemical Technology Consortium (through a Thai governmental loan from the Asian Development Bank), and the Petroleum and Petrochemical College, Chulalongkorn University, Thailand. Ratchanu Buhngachat was acknowledged for her contribution in preparing most of the samples investigated in this work.

6.8 References

[1] S. Suzaki, J. Mizuguchi, Dyes Pigments 61 (2004) 69.

[2] T. Sterzynski, P. Calo, M. Lambla, M. Thomas, Polym. Eng. Sci. 37 (1997) 1917.

[3] J. Broda, Polymer 44 (2003) 1619.

[4] J. Broda, Polymer 44 (2003) 6943.

[5] J. Broda, Crystal Growth Des. 4 (2004) 1277.

[6] J. Broda, J. Appl. Polym. Sci. 90 (2003) 3957.

[7] M. Avrami, J. Chem. Phys. 7 (1939) 1103.

[8] M. Avrami, J. Chem. Phys. 8 (1940) 212.

[9] M. Avrami, J. Chem. Phys. 9 (1941) 177.

[10] Wunderlich, B. in Macromolecular Physics, Vol. 2, Academic Press New York, 1976, pp 147.

[11] P. Supaphol, J. Appl. Polym. Sci. 78 (2000) 338.

[12] Q.X. Zhang, Z.H. Zhang, H.F. Zhang, Z.S. Mo, J. Polym. Sci. Polym. Phys. 40 (2002) 1784.

[13] P. Supaphol, P. Thanomkiat, R.A. Phillips, Polym. Test 23 (2004) 881.

[14] R. Kolb, C. Wutz, N. Stribeck, G. von Krosigk, C. Riekel, Polymer 42 (2001) 5257.